Atmospheric Environment 265 (2021) 118720

Contents lists available at ScienceDirect

Atmospheric Environment

journal homepage: www.elsevier.com/locate/atmosenv

High-volume sampler for size-selective sampling of bioaerosols including viruses

Jun-Hyung Lim [a], Sang Hwan Nam [b], Jongwoo Kim [b], Nam Hoon Kim [b], Gun-Soo Park [b,c], Jin-Soo Maeng [b,c], Se-Jin Yook [a,*]

[a] School of Mechanical Engineering, Hanyang University, Seoul, 04763, South Korea
[b] Center for Convergent Research of Emerging Virus Infection, Korea Research Institute of Chemical Technology, Yuseong, Daejeon, 34114, South Korea
[c] Research Group of Food Processing, Korea Food Research Institute, Wanju, 55365, Jeonbuk, South Korea

HIGHLIGHTS

- We designed 3-stage high-volume bioaerosol sampler with size-selective sampling.
- The sampler draws air at a high flow rate of 1000 L/min.
- We simulated the suspension of bioparticles attached to other particles.
- We analyzed the bioaerosol samples collected in each stage via PCR method.

ARTICLE INFO

Keywords:
Bioaerosol
Size-selective sampler
High-volume sampler
Cyclone separator
Filter

ABSTRACT

Owing to the recent global spread of the new coronavirus SARS-CoV-2, the development of technology to effectively detect viruses in crowded public places is urgently needed. In this study, a three-stage high-volume bioaerosol sampler was developed for the size-selective sampling of bioaerosols through the suction of air at a high flow rate of 1000 L/min. In stage 1, an omnidirectional inlet cyclone separator that can draw air from all directions was applied to collect bioaerosols larger than 10 μm in the collection fluid. In stage 2, an axial flow cyclone separator was used to collect bioaerosols sized between 2.5 and 10 μm in the collection fluid. In stage 3, bioaerosols smaller than 2.5 μm were collected on a filter and extracted in a solution through an elution process using a sodium phosphate buffer. To simulate the suspension of bioparticles including viruses that are attached to other particles in the atmosphere, the aerosol samples were prepared by coagulating aerosolized bacteriophages with Arizona test dust. Then, the coagulated particles were collected for 30 min using the developed bioaerosol sampler, and the samples collected in each stage were analyzed via polymerase chain reaction (PCR) method. The PCR analysis results confirmed that the high-volume bioaerosol sampler enables size-selective bioaerosol sampling even at a high airflow rate of 1000 L/min. The developed high-volume bioaerosol sampler will be useful in detecting viruses through PCR analysis because it can collect bioaerosols within a specific size range.

1. Introduction

Bioaerosols are everywhere in the indoor and outdoor environments, and exposure to bioaerosols of high concentrations may adversely affect human health (Reponen et al., 1994; Meklin et al., 2002; Douwes et al., 2003). Bioaerosols include bacteria, pollen, protein, spores, and viruses, and their size distribution varies significantly depending on their type (Fröhlich-Nowoisky et al., 2016). Most bioaerosols in the atmosphere do not exist independently; rather, they are attached to other aerosol particles (Byeon et al., 2008). Thus, particles containing bioaerosols can be much larger than bioaerosols. For example, although viruses range from 25 nm to 400 nm in diameter, the size of virus-containing respiratory droplets suspended in the air can range from 200 nm to 100 μm (Han et al., 2013). The size range of the virus-containing droplets becomes even larger when the droplets form clusters with other aerosols in the atmosphere (Hirst and Pons, 1973). For efficient collection of such bioaerosols of a wide size range, bioaerosol samplers with collection mechanisms of solid plate impaction, centrifugal impaction, filtration, or liquid impingement are used (Hogan et al., 2005). Each mechanism

* Corresponding author.
E-mail address: ysjnuri@hanyang.ac.kr (S.-J. Yook).

https://doi.org/10.1016/j.atmosenv.2021.118720
Received 30 June 2021; Received in revised form 6 September 2021; Accepted 8 September 2021
Available online 12 September 2021

Abbreviations

polymerase chain reaction (PCR)
computational fluid dynamics (CFD)
Reynolds stress model (RSM)
discrete phase models (DPM)
user-defined function (UDF)

has its own benefits and shortcomings.

Inertial impactors are widely used for bioaerosol sampling and operate based on the solid plate impaction principle. Inertial impactors can predict the cutoff size theoretically, create a sharp collection efficiency curve, and reduce the cutoff size to tens to hundreds of nanometers in a low-pressure operating environment. Inertial impactors facilitate the use of multiple nozzles and multistage configurations in its structure. Many studies have shown that inertial impactors could be successfully used to collect airborne microorganisms by size (Anderson, 1958; Decker and Wilson, 1954; Juozaitis et al., 1994). However, their efficiency can vary depending on the overloading of samples on the impaction plate (Marple and Willeke, 1976). Cyclone separators utilize the centrifugal impaction mechanism and cause less particle bounce and re-entrainment problems. They are mainly used as pre-samplers to selectively remove large particles, because they exhibit a larger cutoff size than inertial impactors and their collection efficiency curve is generally not as sharp (Hering, 1995). Cyclone separators facilitate multistage configurations as they have one inlet and one outlet, and a multistage cyclone system can be used to collect viable organisms in the atmosphere by collecting the particles by size (Smith et al., 1979; Lindsley et al., 2006). However, the use of cyclone separators in series can lengthen the pipe connecting the outlet of one cyclone separator (upstream) and the inlet of another one (downstream), leading to an increase in particle transport loss and an increase in the pressure drop during the operation of the sampler. The filtration mechanism collects aerosols based on interception, diffusion, and electrostatic attraction in addition to inertial impaction, and thus it exhibits higher collection efficiency in a broad particle size range than other methods. Filtration is widely used for bioaerosol sampling because of its high collection efficiency for particles smaller than 1 μm (Aizenberg et al., 2000). Microorganisms collected on filters can be extracted by elution process with more than 90% efficiency (Palmgren et al., 1986). In addition, samplers that use the filtration mechanism can be designed in small sizes (Grinshpun et al., 1995). The liquid impingement method has a high retention efficiency and can achieve a relatively small cutoff size because it directly collects aerosols in the collection fluid. However, the collection performance may vary depending on the sampling time if an evaporating fluid is used as the collection fluid because of the reduction in the volume of the collection fluid with time (Lin et al., 1997). A representative device of the liquid impingement method is the midget impinger developed by Littlefiled et al. (1937) or the BioSampler designed by Willeke et al. (1998). The midget impinger and the BioSampler have been widely used because they do not exhibit overloading problems, and they enable a simple design structure and operation method (Henderson, 1952; May and Harper, 1957; Lin et al., 2000); however, their typical suction flow rate is not appropriate for the high-volume sampling.

The purpose of this study is to develop a high-volume bioaerosol sampler that is compact and portable. In previous studies, samplers with one cutoff size were mainly used; however, the need for size-selective bioaerosol sampling has been consistently highlighted (Hogan et al., 2005). In addition, because the toxicity of bioaerosols can be more lethal when they are introduced into the human respiratory system, a bioaerosol sampler that can collect particles by size according to the size ranges of aerosols accumulated in the organs of the respiratory system is required (Kenny et al., 1998). According to ISO Standard 7708 'Air quality – Particle size fraction definitions for health-related sampling', *inhalable* convention, *thoracic* convention, and *high risk respirable* convention correspond to the aerodynamic diameters of <100 μm, 10 μm, and 2.5 μm, respectively. Based on these definitions, the high-volume bioaerosol sampler developed in this study has three stages (Fig. S1), and it was designed to collect bioaerosols larger than 10 μm in stage 1, bioaerosols sized between 2.5 μm and 10 μm in stage 2, and bioaerosols smaller than 2.5 μm in stage 3. Most of the previously developed samplers were fabricated such that the omnidirectional inlet was separated from the pre-separator (Hsiao et al., 2010), which may increase the complexity of the system. In this study, in order to construct a more compact system, a new type of omnidirectional inlet cyclone separator that can simultaneously perform the functions of the omnidirectional inlet and the pre-separator was applied to stage 1, and an axial flow cyclone separator that can simplify the flow path was employed in stage 2.

2. Materials and methods

2.1. Design of high-volume bioaerosol sampler

The developed high-volume bioaerosol sampler has four blocks (Fig. S1). A vertical flow path from top to bottom was designed for the structure of the entire system to be compact while minimizing the particle transport loss during the transport of aerosols. Fig. S2 shows the detailed geometry of the interior of the high-volume bioaerosol sampler, and the dimensions of the main parts are summarized in Table S1. As shown in the top right corner of Fig. S2, 16 guide vanes with a specific angle were installed at the inlet of the omnidirectional inlet cyclone separator to allow aerosols to be introduced from all directions and to immediately generate rotating airflow inside. The omnidirectional inlet cyclone separator used in stage 1 was designed to have a cutoff size of 10 μm for an operating flow rate of 1000 L/min (Lim et al., 2021). An axial flow cyclone separator was employed in stage 2 to allow aerosols to flow from top to bottom, and it was designed to have a cutoff size of 2.5 μm for an operating flow rate of 1000 L/min. The collection fluid was contained in the dust hopper of each cyclone separator, and the dust hopper was designed to prevent the collection fluid from overflowing by swirling flow and flowing into the next stage. In stage 3, a filter holder was used to install a filter in circular shape with a diameter of 60 mm (bottom right corner of Fig. S2). Particles escaping stages 1 and 2 were finally collected on a filter.

2.2. Numerical method

To predict the performance of the cyclone separators applied to stages 1 and 2 of the developed high-volume bioaerosol sampler, numerical analysis was conducted using ANSYS FLUENT *Release 16.1*, a commercial computational fluid dynamics (CFD) code. The flow was assumed to be steady, incompressible, and turbulent. The Reynolds stress model (RSM), which is suitable to analyze the characteristics of turbulent flow in the form of a vortex, was selected because it exhibits higher accuracy than other turbulence models in predicting the flow distribution inside a cyclone separator (Kaya and Karagoz, 2008; Shukla et al., 2011). Table S2 lists the numerical schemes used for this study. Since the collection fluid was used in cyclone separators, an analysis was conducted for multiphase flow in which air and water coexisted. The Eulerian model was used as a multiphase model, because the behavior of gas and liquid inside a cyclone separator can be well simulated when both the RSM turbulence model and Eulerian multiphase model are used for cyclone analysis under multiphase flow conditions (Cokljat et al., 2006). The boundary conditions for the flow analysis are listed in Table S3. The aerosol suction rate was set to 1000 L/min. The properties of air and water were set at the temperature of 300 K and pressure of 101.3 kPa.

Upon completion of the flow analysis, the behavior of aerosol particles was analyzed using discrete phase models (DPM), a built-in function of FLUENT, to predict the cutoff sizes of the cyclone separators applied to stages 1 and 2. A one-way gas–particle interaction was applied under the assumption that particles could not affect the flow of air but the flow could affect the behavior of particles, because the number concentration of aerosol particles introduced into cyclone separators was sufficiently low. It was assumed that the particles had a perfectly spherical shape, and the density of the particles was 1000 kg/m^3 (*i.e.*, aerodynamic diameter). The forces considered for the analysis of particle behavior were the gravitational force, drag force, Brownian force, and Saffman lift force. The random walk model was applied considering the influence of turbulence inside cyclone separators. Considering that the collection fluid was contained in the cyclone dust hopper, boundary conditions were set so that particles could be trapped when the particle trajectory calculated by DPM passed through the mesh cell where the volume fraction of the collection fluid (water) exceeded 50%. To implement the boundary conditions, a user-defined function (UDF) was coded. The grid independence test was conducted while the number of grids was varied from 0.5 to 2.0 million, and it was confirmed that changes in pressure drop and cutoff size were less than 2.6% and 3.2%, respectively. Therefore, the number of grids was determined to be approximately 0.5 million for the analysis of the omnidirectional inlet cyclone separator in stage 1 and 0.8 million for the analysis of the axial flow cyclone separator in stage 2.

2.3. Experimental method

Fig. S3 shows the experimental setup used to evaluate the performance of the high-volume bioaerosol sampler. Because the sampling inlet was located at the top of the high-volume bioaerosol sampler, an experiment was performed by exposing only the inlet section in the 700 mm × 700 mm × 700 mm test chamber. The operating flow rate of the sampler was fixed at 1000 L/min, and the flow rate was measured using a pitot tube located inside block 4. A differential pressure transmitter (CP 210, KIMO, Montpon, Dordogne, France) was connected to the pressure taps installed at the inlet and outlet of each stage to measure the pressure drop for each stage. Particle-free air was introduced into the test chamber through a high-efficiency particulate air (HEPA) filter installed at the top of the test chamber. A tube for injecting aerosols was located in the upper part of the test chamber, and a fan was used to evenly spread the aerosol in the test chamber. The Arizona test dust (ISO 12103–1, A4 type) was aerosolized using a solid aerosol generator (SAG 410, TOPAS, Dresden, Saxony, Germany) and introduced into the test chamber after mixing with particle-free air in the dilution chamber. An optical particle counter (OPC; Model 1.109, GRIMM, Ainring, Bayern, Germany) was used to measure the aerosol number concentrations in the test chamber and the sampler. The particle size measured by the OPC was converted into the aerodynamic size, using density (ρ_p = 2.56 g/cm^3) and dynamic shape factor (κ = 1.4) of the Arizona test dust (Fletcher and Bright, 2000).

To measure the collection efficiency of stage 1, a geometry that combined blocks 1, 2, and 4 was used, and the guide vanes were removed from block 2. The geometry that combined blocks 2, 3, and 4 was used to measure the collection efficiency of stage 2; the guide vanes were installed in block 2, but no filter was installed in stage 3. To measure the collection efficiency of stage 3, only the filter holder and block 4 were connected; two circular tubes with the same diameter as the filter were placed before and after the filter holder. Isokinetic sampling probes with thin wall and sharp-edged tip were used upstream and downstream of each stage to improve the accuracy of the number concentration measurement. Pitot tubes were used to measure the airflow speed at the positions where the isokinetic sampling probes were placed, and the speed of the aerosols introduced into the isokinetic sampling probes was adjusted to be equal to the speed of the surrounding airflow. The collection efficiency (η) was calculated using Eq. (1). Here, C_{up} and C_{down} are the aerosol number concentrations measured upstream and downstream of each stage, respectively.

$$\eta = 1 - \frac{C_{down}}{C_{up}} \quad (1)$$

Then, an experiment was performed using bacteriophages to evaluate the performance of the high-volume bioaerosol sampler in collecting bioaerosols. Bacteriophage T4 was propagated according to the Phase on Tap protocol (Bonilla et al., 2016). The solution obtained by diluting a bacteriophage sample with phosphate-buffered saline at a ratio of 1:10 was sprayed using a Collison type atomizer (AG-01, HCT, Icheon, Republic of Korea). This method has been widely used to generate bioaerosols artificially. The droplets generated by the Collison type atomizer generally become smaller than 1 μm as they are dried (Niazi et al., 2021). The use of bacteriophages smaller than 1 μm creates a situation significantly different from reality because bioaerosols in the atmosphere and indoor air mostly exist in combination with particles of irregular sizes. Therefore, to simulate the actual situation more closely, bacteriophage-containing aerosols generated using the atomizer and diffusion dryer were mixed with Arizona test dust aerosols in a dilution chamber, with sufficient residence time to induce the coagulation of bacteriophages with Arizona test dust particles. Mixed aerosols were introduced into the test chamber and drawn using a high-volume bioaerosol sampler at a flow rate of 1000 L/min for 30 min. The uniformity of particle concentration in the test chamber was checked by measuring aerosol number concentrations at 4 different positions, *i.e.*, at 0°, 90°, 180°, and 270° in the circumferential direction, on an imaginary plane located at the same level as the omnidirectional inlet. The relative difference in the measured number concentrations was lower than 2%, indicating that the particles were evenly dispersed in the test chamber. Each dust hopper of stages 1 and 2 contains 50 mL of the collection fluid (sodium phosphate buffer). The reason why the sodium phosphate buffer was used as the collection fluid was because its ion concentration and osmotic pressure are very similar to those of the human body and thus it is helpful for maintaining bacteriophage viability and also because it can be produced in large quantities easily. A filter sheet was installed in the filter holder of stage 3 for the collection experiment. Upon completion of sampling, each collection fluid of stages 1 and 2 was drained and placed in separate containers. The filter of stage 3 was eluted using the sodium phosphate buffer to extract the bioaerosols collected on the filter, and the bioaerosols were placed in another container. Using a real-time PCR detection system (CFX96 Touch System, Bio-Rad, CA, USA), PCR analysis was conducted for bioaerosol samples collected in each stage to measure the collected bacteriophage concentrations.

3. Results and discussion

Fig. 1 shows the simulation results of air velocity magnitude contours, water volume fraction distribution, and particle trajectories inside the omnidirectional inlet cyclone separator used in stage 1. The air from the outside rotated around the central axis as it was introduced through the gaps between the guide vanes and accelerated at the same time (Fig. 1(a)). When the operating flow rate was 1000 L/min, the maximum speed of the airflow inside the cyclone separator was 22.9 m/s. The airflow inside the dust hopper was relatively low because of the influence of the collection fluid contained in the dust hopper. The collection fluid rotated in the same direction as the rotating airflow, with a velocity of 3 m/s or less, which was significantly lower than the velocity of the surrounding air (Fig. 1(a)), and 50 mL of the collection fluid remained in the dust hopper without overflowing while rotating (Fig. 1(b)). Fig. 1(c) shows the trajectory of 10-μm-sized particles. The particles were predicted to rotate immediately after being introduced through the gaps between the guide vanes. Half of them were collected in the collection fluid contained in the dust hopper and the other half escaped through the outlet at the bottom. Here, the trajectory of the collected particles

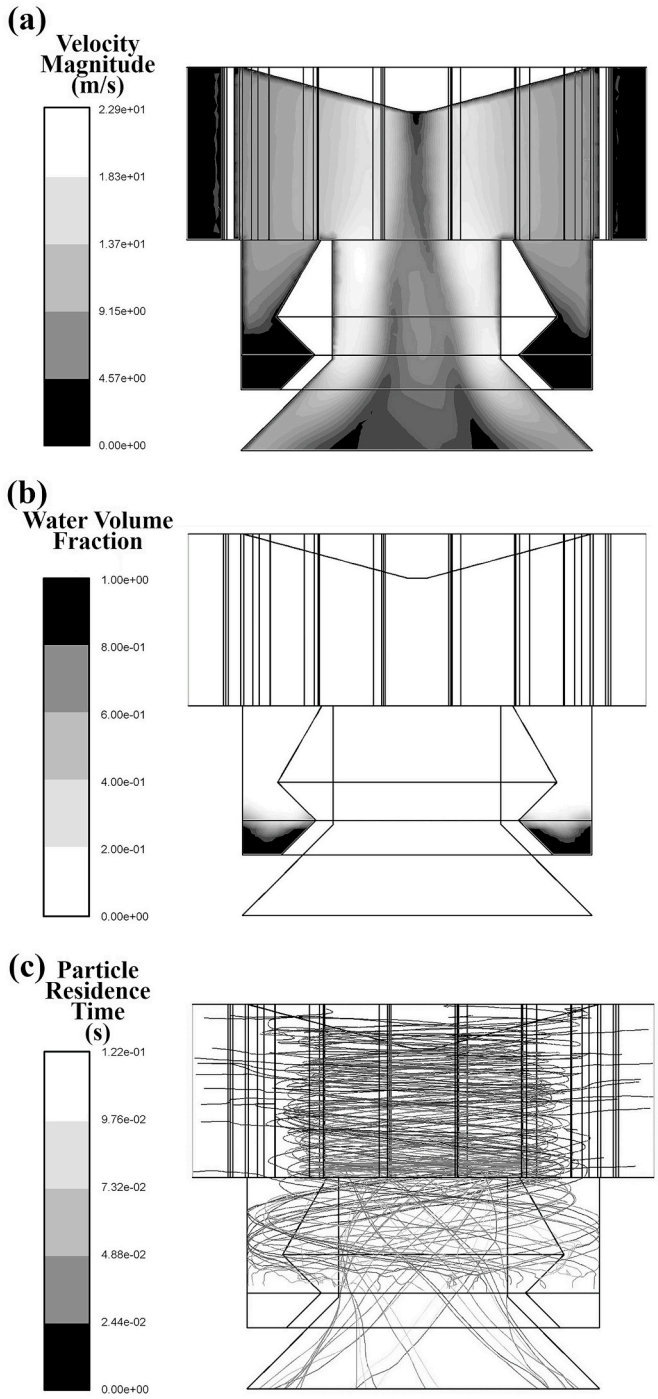

Fig. 1. Velocity magnitude (a), water volume fraction (b), and particle trajectory (c) of stage 1, omnidirectional cyclone separator.

appears to end in the middle area without reaching the bottom of the dust hopper, because the condition, in which particles were trapped when they passed through the mesh cell of the water volume fraction exceeding 50%, was applied by the UDF coded for this analysis.

Fig. 2 shows the simulation results of air velocity magnitude contour, water volume fraction distribution, and particle trajectories inside the axial flow cyclone separator applied to stage 2. The airflow introduced from the top of stage 2 formed a rotating airflow around the central axis as it passed through the guide vanes, and a maximum airflow velocity of 50.9 m/s was predicted at the entrance of the outlet tube (Fig. 2(a)). As in stage 1, the air velocity in the dust hopper of stage 2 was lower than that in other areas owing to the influence of the collection fluid. The collection fluid also rotated inside the dust hopper under the influence of the rotating airflow at a relatively low speed of approximately 6 m/s or less (Fig. 2(a)). A total of 50 mL of the collection fluid contained in the dust hopper remained in the dust hopper without overflowing during the operation of the cyclone separator (Fig. 2(b)). Fig. 2(c) shows the trajectory of 2.5-μm-sized particles. The particles introduced from the top of the cyclone separator rotated along with the airflow as they passed through the guide vanes, and most of them were observed near the inner wall of the cyclone cylinder owing to the centrifugal force. Approximately half of the particles were predicted to be collected in the collection fluid contained in the dust hopper as they descended along the inner wall, and the other half escaped through the outlet at the bottom of the cyclone separator.

Fig. 3 shows the collection efficiency of stages 1–3. For cyclone separators in stages 1 and 2, both experiments and simulations were conducted. In stage 1, in which the omnidirectional inlet cyclone separator was used, the simulation results were in good agreement with the experimental results, with an error of 12% or less. The cutoff size was 10 μm, and most particles larger than 18 μm could be collected. In stage 2, in which the axial flow cyclone separator was used, the simulation results were in good agreement with the experimental results with an error of less than 10%. The cutoff size was 2.5 μm, and most particles larger than 6 μm could be collected. In stage 3, only an experiment was conducted. To meet the high operating flow conditions of the high-volume bioaerosol sampler, it is necessary to use a filter that has high air permeability and that can collect particles with high efficiency. When an experiment was performed after installing various types of filters, including paper filter, melt blown filter, quartz filter, membrane filter, and cotton filter, in the filter holder of stage 3, only the melt blown filter and cotton filter could meet the operating flow rate condition of 1000 L/min when the vacuum motor with 1500 W power was installed in the block 4 of the high-volume bioaerosol sampler. Because the collection efficiency of the cotton filter was measured to be lower than that of the melt blown filter, the melt blown filter was finally selected. In this study, one of the melt blown filters, the certified Korea Filter 80 (KF80), which is typically used as a material for medical face masks, was used. Although the face velocity of the aerosols that passed through the filter was relatively high (10.9 m/s) at an operating flow rate of 1000 L/min, KF80 exhibited a collection efficiency of 93.7% for a particle size of 0.34 μm (Fig. 3). The collection efficiency increased as the particle size increased, reaching 100% for particles larger than 1.8 μm.

Most studies on multi-stage samplers measured the collection efficiency of each stage and predicted the size range of the particles to be sampled in each stage when all the stages were used (May, 1966; Noll, 1970; Smith et al., 1979; Hsiao et al., 2010). In this study, the fraction of sampled particles in each stage was also predicted for particles introduced into the high-volume bioaerosol sampler when all stages were considered to be connected based on the collection efficiency data of each stage shown in Fig. 3, and the results are presented in Fig. 4. Here, the particle transport loss that might occur at the junctions between neighboring stages was not considered. Among the particles introduced into the high-volume bioaerosol sampler, those larger than 10 μm are likely to be collected in stage 1, those sized between 2.5 and 10 μm in stage 2, and those smaller than 2.5 μm in stage 3.

Fig. 5(a) and (b) show the number and mass concentrations of aerosols measured near the omnidirectional inlet of the high-volume bioaerosol sampler operating in the test chamber, when the bacteriophage-containing aerosols and Arizona test dust aerosols were mixed in the dilution chamber and then injected into the test chamber. Here, the number concentration measured using the OPC was converted into the mass concentration. Considering the results of Niazi et al. (2021), most of the sizes of bacteriophage aerosol, generated using the Collison type atomizer and dried using the diffusion dryer in this study, were expected to be smaller than 1 μm. However, as shown in Fig. 5(a), particles of various sizes were present in the size group of ≤10 μm, because the bacteriophage aerosol was mixed with the Arizona test dust

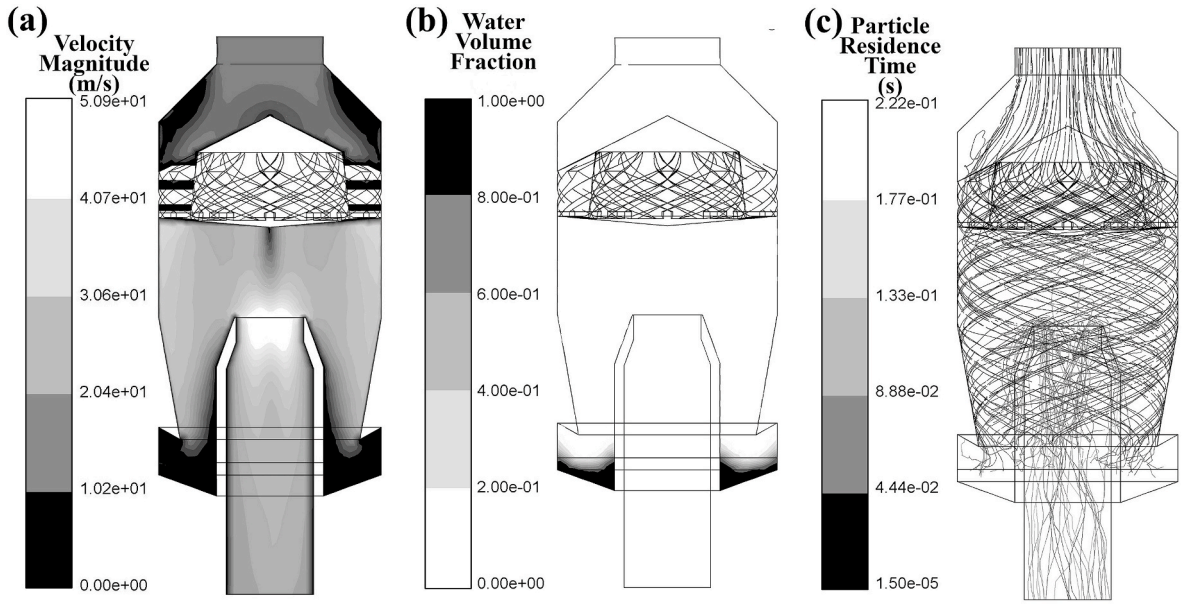

Fig. 2. Velocity magnitude (a), water volume fraction (b), and particle trajectory (c) of stage 2, axial flow cyclone separator.

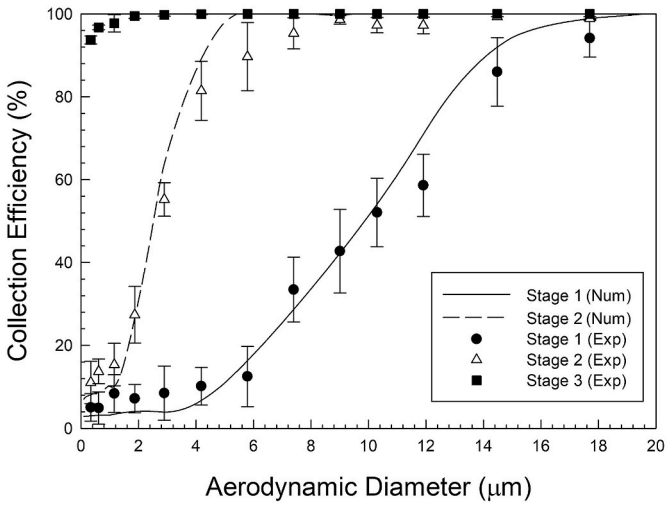

Fig. 3. Collection efficiency of individual stages of the high-volume bioaerosol sampler (each experiment was repeated 3 times and error bars show standard deviations).

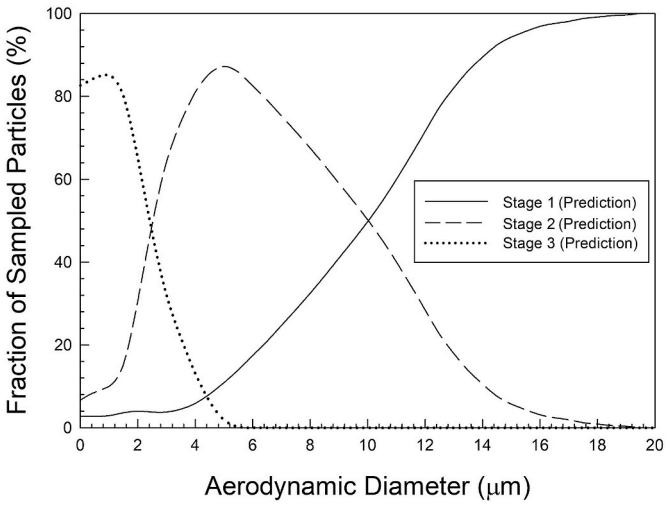

Fig. 4. Relative collection efficiency of all stages of high-volume bioaerosol sampler.

aerosol. As displayed in Fig. 5(b), a bimodal distribution was observed with a low peak at around 0.7 μm and a high peak at 4 μm. It was assumed that this distribution can approximately simulate the size distribution of the aerosols in the atmosphere. Aerosols with this mass concentration were sampled for 30 min using the high-volume bioaerosol sampler. Then, PCR analysis was conducted on the bioaerosol samples collected in each stage.

Fig. 6 shows the fraction of the collected bacteriophages in each stage compared to the total mass of the bacteriophages collected in all stages of the high-volume bioaerosol sampler. Here, the predictions were obtained for particles with all sizes collected in each stage by multiplying the mass concentration shown in Fig. 5(b) by the fraction of sampled particles shown in Fig. 4. The predicted fractions were 8.8% in stage 1, 61.5% in stage 2, and 29.7% in stage 3. It should be noted that these prediction values are irrelevant to the bioaerosols collected in each stage due to the unknown size distribution of bacteriophage-containing aerosol. On the other hand, experiments were performed with or without mixing the bacteriophage aerosol with the Arizona test dust. When only the bacteriophage aerosol was introduced into the test chamber, *i.e.*, without the Arizona test dust, the fractions of collected bacteriophages were 1.6% in stage 1, 8.9% in stage 2, and 89.5% in stage 3, meaning that most of the bacteriophage-containing particles had the aerodynamic sizes smaller than 2.5 μm. This was mainly because most of bacteriophages aerosolized using a Collison type atomizer and dried using a diffusion dryer were expected to be smaller than 1 μm, based on the results of Niazi et al. (2021). When the bacteriophage aerosol was mixed with the Arizona test dust and then introduced into the test chamber, the fractions of collected bacteriophages were 4.8% in stage 1, 41.4% in stage 2, and 53.8% in stage 3. In other words, bacteriophages were collected in stages 1 and 2, of which cutoff sizes were 10 μm and 2.5 μm, respectively, with higher fractions compared to the case without the Arizona test dust. This clearly implies that the bacteriophages, to some extent, were coagulated with the Arizona test dust particles and the bacteriophages attached to large dust particles were collected in cyclone separators owing to the aerodynamic size of coagulated particles. For both the predicted and experimental results, the smallest amount of bioaerosols was collected in stage 1, while much larger

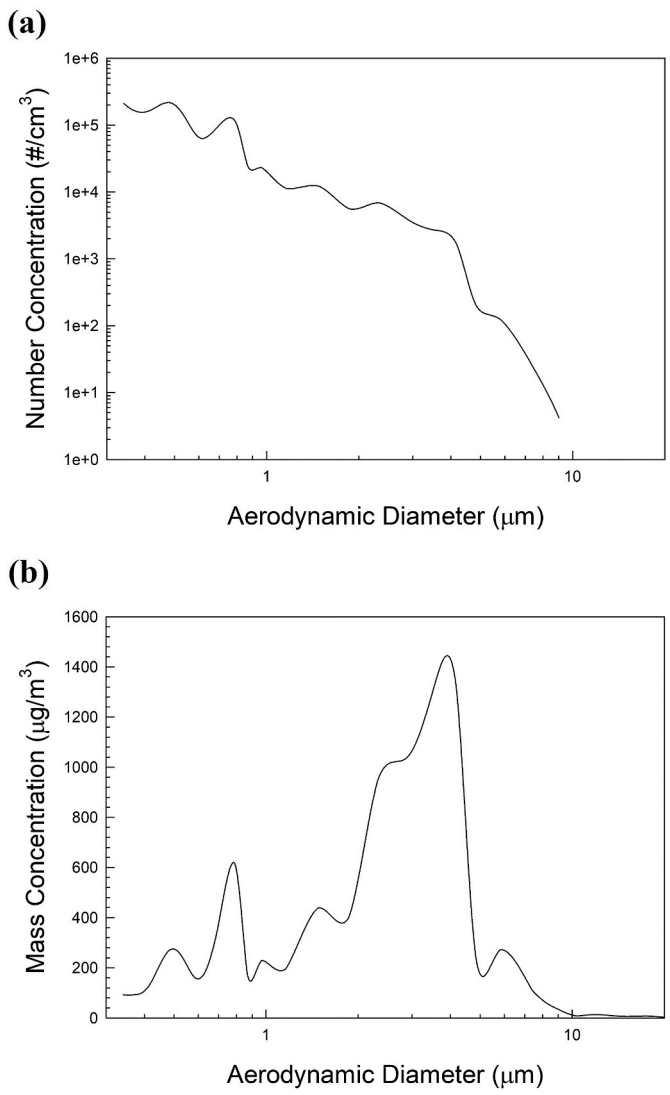

Fig. 5. Number distribution (a), mass distribution (b), of test aerosol sampled at the test chamber.

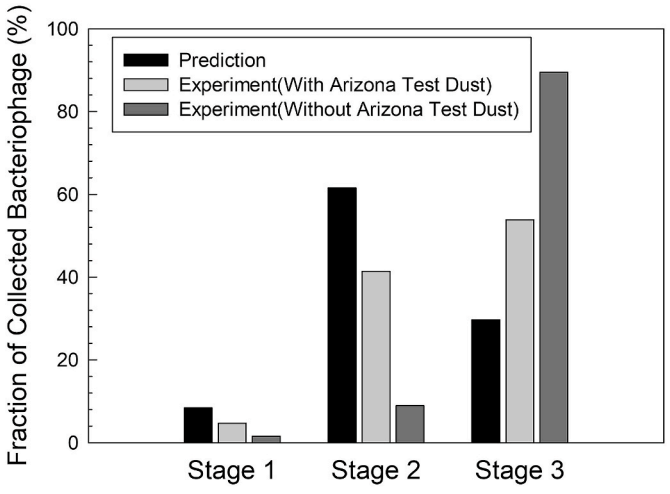

Fig. 6. Relative collected bacteriophage percentage of the high-volume bioaerosol sampler.

amounts were collected in stages 2 and 3. The stages 2 and 3 showed differences in the collected bioaerosol mass between the predicted and experimental results. This might be because the bacteriophage-containing aerosols and Arizona test dust aerosols did not perfectly coagulate in the dilution chamber, and thus more particles containing bacteriophages existed in the ≤2.5 μm size group. The experimental results in Fig. 6 show that bacteriophage-containing particles can be successfully collected in the collection fluid contained in stages 1 and 2 and detected through PCR analysis even when they exist in the form of aerosols larger than 1 μm through coagulation with Arizona test dust particles. Despite the differences between the predicted and experimental results in Fig. 6, the developed high-volume bioaerosol sampler can be very useful in collecting bioaerosols by size through the suction of air at a high flow rate of 1000 L/min.

Fig. 7 shows the numerical analysis and experimental results for the pressure drop in each stage. In stage 3, only the experimental results are shown because the simulation was not performed. In stages 1 and 2, the pressure drops were predicted to be 460 and 2357 Pa, respectively, via numerical analysis, and they were measured to be 615 and 2632 Pa in the experiment, showing a relatively good agreement between the numerical and experimental results. The pressure drops measured in the experiment were slightly higher than those predicted via numerical analysis because the junctions between the neighboring stages were not considered in the numerical analysis. In stage 3, the pressure drop was measured as 7832 Pa in the experiment. Therefore, when the operating flow rate was 1000 L/min, the total pressure drop through the three stages was approximately 11,000 Pa.

4. Conclusion

In this study, for size-selective sampling of bioaerosols including viruses in large and crowded public places, a three-stage high-volume bioaerosol sampler capable of collecting bioaerosols by size through the suction of air at a high flow rate of 1000 L/min was developed. An omnidirectional inlet cyclone separator capable of drawing air from all directions was applied to stage 1, and the cyclone separator was designed for a cutoff size of 10 μm. An axial flow cyclone separator with a cutoff size of 2.5 μm was designed and applied to stage 2. The collection fluid (50 mL) was contained in the dust hopper of the cyclone separators used in stages 1 and 2 to collect bioaerosols in the collection fluid. In stage 3, a filter holder was designed and installed so that a circular filter sheet with a diameter of 60 mm could be installed. Bioaerosols collected on the filter were extracted in a solution through an elution process that used a sodium phosphate buffer. To minimize the particle transport loss inside the sampler, the flow path was simplified as much as possible so that the air drawn into the inlet could flow from top

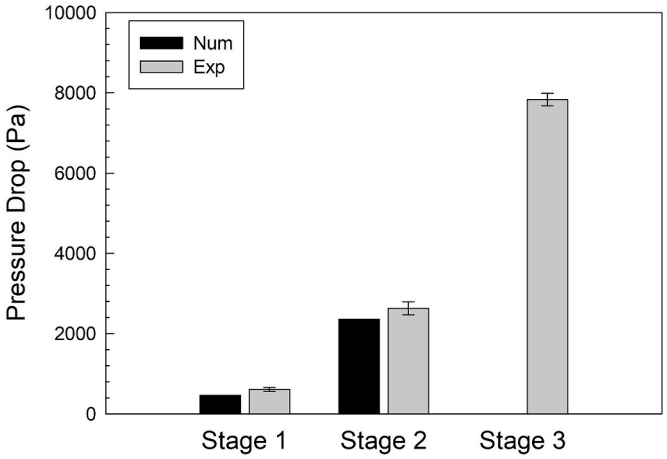

Fig. 7. Pressure drop of the high-volume bioaerosol sampler.

to bottom until it reached the vacuum motor. Experiments were conducted by inducing the coagulation of bacteriophage-containing aerosols with Arizona test dust aerosols (mixed aerosols) to simulate an actual situation in which bioaerosols, such as viruses, are suspended in the atmosphere by attaching to other particles. The artificially generated bioaerosols exhibited a bimodal distribution similar to that of the actual atmospheric aerosols. The mixed aerosols were sampled for 30 min using the high-volume bioaerosol sampler, and the samples collected in each stage were analyzed using the PCR method. The effective detection of bioaerosols collected in each stage by size via PCR analysis confirmed that the high-volume bioaerosol sampler enables size-selective bioaerosol sampling even at a high airflow rate of 1000 L/min. The developed bioaerosol sampler has advantages of high-volume size-selective sampling, compact and portable design, and easy and fast assembly and disassembly, etc. Therefore, the developed high-volume bioaerosol sampler is expected to be very useful in effectively sampling bioaerosols and detecting viruses through PCR analysis by drawing air at a high flow rate in crowded public places. In future studies, the developed high-volume bioaerosol sampler needs to be compared with other existing bioaerosol samplers for bioaerosol exposure assessment.

CRediT authorship contribution statement

Jun-Hyung Lim: Investigation, Data curation, Software, Writing – original draft. **Sang Hwan Nam:** Conceptualization, Methodology. **Jongwoo Kim:** Investigation, Validation. **Nam Hoon Kim:** Investigation, Validation. **Gun-Soo Park:** Investigation, Data curation. **Jin-Soo Maeng:** Funding acquisition. **Se-Jin Yook:** Conceptualization, Methodology, Supervision, Writing – review & editing.

Declaration of competing interest

The authors declare that they have no known competing financial interests or personal relationships that could have appeared to influence the work reported in this paper.

Acknowledgment

This work was supported by the National Research Council of Science & Technology grant by the Korean government (MSIP) (No. CRC-16-01-KRICT).

Appendix A. Supplementary data

Supplementary data to this article can be found online at https://doi.org/10.1016/j.atmosenv.2021.118720.

References

Aizenberg, V., Grinshpun, S.A., Willeke, K., Smith, J., Baron, P.A., 2000. Performance characteristics of the button personal inhalable aerosol sampler. Am. Ind. Hyg. Assoc. J. 61, 398–404. https://doi.org/10.1080/15298660008984550.

Andersen, A.A., 1958. New sampler for the collection, sizing, and enumeration of viable airborne particles. J. Bacteriol. 76, 471–484. https://doi.org/10.1128/JB.76.5.471-484.1958.

Bonilla, N., Rojas, M.I., Cruz, G.N.F., Hung, S.H., Rohwer, F., Barr, J.J., 2016. Phage on tap–a quick and efficient protocol for the preparation of bacteriophage laboratory stocks. PeerJ 4, e2261. https://doi.org/10.7717/peerj.2261.

Byeon, J.H., Park, C.W., Yoon, K.Y., Park, J.H., Hwang, J., 2008. Size distributions of total airborne particles and bioaerosols in a municipal composting facility. Bioresour. Technol. 99, 5150–5154. https://doi.org/10.1016/j.biortech.2007.09.014.

Cokljat, D., Slack, M., Vasquez, S.A., Bakker, A., Montante, G., 2006. Reynolds-stress model for Eulerian multiphase. Prog. Comput. Fluid Dyn., Int. J. 6, 168–178. https://doi.org/10.1504/PCFD.2006.009494.

Decker, H.M., Wilson, M.E., 1954. A slit sampler for collecting air-borne microorganisms. Appl. Microbiol. 2, 267–269. https://doi.org/10.1128/AM.2.5.267-269.1954.

Douwes, J., Thorne, P., Pearce, N., Heederik, D., 2003. Bioaerosol health effects and exposure assessment: progress and prospects. Ann. Occup. Hyg. 47, 187–200. https://doi.org/10.1093/annhyg/meg032.

Fletcher, R.A., Bright, D.S., 2000. Shape factors of ISO 12103-A3 (medium test dust). Filtr. Sep. 37, 48–56. https://doi.org/10.1016/S0015-1882(00)80200-1.

Fröhlich-Nowoisky, J., Kampf, C.J., Weber, B., Huffman, J.A., Pöhlker, C., Andreae, M. O., Lang-Yona, N., Burrows, S.M., Gunthe, S.S., Elbert, W., Su, H., Hoor, P., Thines, E., Hoffmann, T., Després, V.R., Pöschl, U., 2016. Bioaerosols in the Earth system: climate, health, and ecosystem interactions. Atmos. Res. 182, 346–376. https://doi.org/10.1016/j.atmosres.2016.07.018.

Grinshpun, S.A., Willeke, K., Kalatoor, S., Baron, P., 1995. Development and evaluation of an aerosol monitor with low wind sensitivity and uniform filter deposition. J. Aerosol Sci. 26, S187–S188. https://doi.org/10.1016/0021-8502(95)97001-U.

Han, Z.Y., Weng, W.G., Huang, Q.Y., 2013. Characterizations of particle size distribution of the droplets exhaled by sneeze. J. R. Soc. Interface 10, 20130560. https://doi.org/10.1098/rsif.2013.0560.

Henderson, D.W., 1952. An apparatus for the study of airborne infection. Epidemiol. Infect. 50, 53–68. https://doi.org/10.1017/S0022172400019422.

Hering, S.V., 1995. Impactors, cyclones, and other inertial and gravitational collectors. In: Cohen, B.S., Hering, S.V. (Eds.), Air Sampling Instruments, eighth ed. American Conference of Governmental Industrial Hygienists, Cincinnati, pp. 279–321.

Hirst, G.K., Pons, M.W., 1973. Mechanism of influenza recombination: II. Virus aggregation and its effect on plaque formation by so-called noninfective virus. Virology 56, 620–631. https://doi.org/10.1016/0042-6822(73)90063-9.

Hogan Jr., C.J., Kettleson, E.M., Lee, M.H., Ramaswami, B., Angenent, L.T., Biswas, P., 2005. Sampling methodologies and dosage assessment techniques for submicrometre and ultrafine virus aerosol particles. J. Appl. Microbiol. 99, 1422–1434. https://doi.org/10.1111/j.1365-2672.2005.02720.x.

Hsiao, T.C., Chen, D.R., Li, L., Greenberg, P., Street, K.W., 2010. Development of a multi-stage axial flow cyclone. Aerosol Sci. Technol. 44, 253–261. https://doi.org/10.1080/02786820903575394.

Juozaitis, A., Willeke, K., Grinshpun, S.A., Donnelly, J., 1994. Impaction onto a glass slide or agar versus impingement into a liquid for the collection and recovery of airborne microorganisms. Appl. Environ. Microbiol. 60, 861–870. https://doi.org/10.1128/AEM.60.3.861-870.1994.

Kaya, F., Karagoz, I., 2008. Performance analysis of numerical schemes in highly swirling turbulent flows in cyclones. Curr. Sci. 94, 1273–1278. https://www.jstor.org/stable/24100235.

Kenny, L.C., Stancliffe, J.D., Crook, B., Stagg, S., Griffiths, W.D., Stewart, I.W., Futter, S. J., 1998. The adaptation of existing personal inhalable aerosol samplers for bioaerosol sampling. Am. Ind. Hyg. Assoc. J. 59, 831–841. https://doi.org/10.1080/15428119891011009.

Lim, J.H., Oh, S.H., Kang, S., Lee, K.J., Yook, S.J., 2021. Development of cutoff size adjustable omnidirectional inlet cyclone separator. Separ. Purif. Technol. 276, 119397 https://doi.org/10.1016/j.seppur.2021.119397.

Lin, X., Willeke, K., Ulevicius, V., Grinshpun, S.A., 1997. Effect of sampling time on the collection efficiency of all-glass impingers. Am. Ind. Hyg. Assoc. J. 58, 480–488. https://doi.org/10.1080/15428119791012577.

Lin, X., Reponen, T., Willeke, K., Wang, Z., Grinshpun, S.A., 2000. Trunov, M. Survival of airborne microorganisms during swirling aerosol collection. Aerosol Sci. Technol. 32, 184–196. https://doi.org/10.1080/027868200303722.

Lindsley, W.G., Schmechel, D., Chen, B.T., 2006. A two-stage cyclone using microcentrifuge tubes for personal bioaerosol sampling. J. Environ. Monit. 8, 1136–1142. https://doi.org/10.1039/b609083d.

Littlefield, J.B., Feicht, F.L., Schrenk, H.H., 1937. Bureau of Mines Midget Impinger for Dust Sampling. US Department of the Interior, Bureau of Mines.

Marple, V.A., Willeke, K., 1976. Inertial impactors: theory, design and use. In: Liu, B.Y.H. (Ed.), Fine Particles, Aerosol Generation, Measurement, Sampling, and Analysis. Academic Press, pp. 411–446. https://doi.org/10.1016/B978-0-12-452950-2.50023-3.

May, K.R., Harper, G.J., 1957. The efficiency of various liquid impinger samplers in bacterial aerosols. Br. J. Ind. Med. 14, 287–297. https://doi.org/10.1136/oem.14.4.287.

May, K.R., 1966. Multistage liquid impinge. Bacteriol. Rev. 30, 559–570. https://doi.org/10.1128/BR.30.3.559-570.1966.

Meklin, T., Reponen, T., Toivola, M., Koponen, V., Husman, T., Hyvärinen, A., Nevalainen, A., 2002. Size distributions of airborne microbes in moisture-damaged and reference school buildings of two construction types. Atmos. Environ. 36, 6031–6039. https://doi.org/10.1016/S1352-2310(02)00769-0.

Niazi, S., Philp, L.K., Spann, K., Johnson, G.R., 2021. Utility of three nebulizers in investigating the infectivity of airborne viruses. Appl. Environ. Microbiol. 87 e00497-21. https://journals.asm.org/doi/abs/10.1128/AEM.00497-21.

Noll, K.E., 1970. A rotary inertial impactor for sampling giant particles in the atmosphere. Atmos. Environ. 4, 9–19. https://doi.org/10.1016/0004-6981(70)90050-8.

Palmgren, U., Ström, G., Blomquist, G., Malmberg, P., 1986. Collection of airborne micro-organisms on Nuclepore filters, estimation and analysis—CAMNEA method. J. Appl. Bacteriol. 61, 401–406. https://doi.org/10.1111/j.1365-2672.1986.tb04303.x.

Reponen, T., Hyvärinen, A., Ruuskanen, J., Raunemaa, T., Nevalainen, A., 1994. Comparison of concentrations and size distributions of fungal spores in buildings with and without mould problems. J. Aerosol Sci. 25, 1595–1603. https://doi.org/10.1016/0021-8502(94)90227-5.

Shukla, S.K., Shukla, P., Ghosh, P., 2011. Evaluation of numerical schemes using different simulation methods for the continuous phase modeling of cyclone

separators. Adv. Powder Technol. 22, 209–219. https://doi.org/10.1016/j.apt.2010.11.009.
Smith, W.B., Wilson, R.R., Harris, D.B., 1979. A five-stage cyclone system for in situ sampling. Environ. Sci. Technol. 13, 1387–1392. https://doi.org/10.1021/es60159a016.
Willeke, K., Lin, X., Grinshpun, S.A., 1998. Improved aerosol collection by combined impaction and centrifugal motion. Aerosol Sci. Technol. 28, 439–456. https://doi.org/10.1080/02786829808965536.